Size-Dependent Analysis for FG-CNTRC Nanoplates Based on Refined Plate Theory and Modified Couple Stress

Cuong-Le Thanh[1,2(✉)], T. Vu-Huu[1], P. Phung-Van[1], Hung Nguyen-Xuan[3], and Magd Abdel Wahab[1]

[1] Soete Laboratory, Faculty of Engineering and Architecture, Ghent University, Ghent, Belgium
cuong.lt@ou.edu.vn
[2] Faculty of Civil Engineering and Electricity, Ho Chi Minh City Open University, Ho Chi Minh City, Vietnam
[3] Center for Interdisciplinary Research in Technology, Ho Chi Minh City University of Technology (Hutech), Ho Chi Minh City, Vietnam

Abstract. This paper presents static bending behaviour of functionally graded carbon nanotube-reinforced composite (FG-CNTRC) nanoplates with four types of distribution of carbon nanotubes. The NURBS based isogeometric analysis (IGA) is associated with refined plate theory (RPT) with four unknowns, in which, there is no need to use shear correction factors. To capture the size-dependent effect of plate, the modified couple stress theory is used with only one material length scale parameter. The accuracy and efficiency of proposed method are demonstrated through comparison with reference solutions. A number of numerical examples are presented to demonstrate the influence of the length scale on the bending behaviors of FG-CNTRC nanoplates.

Keywords: NURBS · FG-CNTRC · RPT · Size-effect · Length scale ratio
Modified couple stress

1 Introduction

In recent year, the functionally graded carbon nanotube-reinforced composites (FG-CNTRC) have paid special attention to many researcher because of superior feature of carbon nanotubes (CNTs), such as high tensile strength, low density, advanced mechanical and electrical properties [2, 4, 8]. Due to the excellent properties of CNT, various applications of FG-CNTRC can be performed in engineering structures such as automobiles, submarine, fuel tanks, diesel engine pistons, aerospace equipment's, solar panels and so on.

To analyse the behaviour of FG-CNTRC beams and plates, many theories are developed to calculate the static bending, vibration and buckling. Based on Finite Element Method (FEM), Rashidifar and Ahmadi [16] investigated the free vibration response of FG nanocomposite beams reinforced single walled carbon nanotubes (SWCNTs). The material properties of FG-CNTRC beam were investigated by using the Eshelby-Mori-Tanaka method. Natural frequencies and critical buckling load of

M. Abdel Wahab (Ed.): NME 2018, LNCE 20, pp. 225–237, 2019.
https://doi.org/10.1007/978-981-13-2405-5_19

FG-CNTRC nanocomposite Timoshenko beams were investigated by Yas and Samadi [24] with different boundary conditions. To analyse the nonlinear vibration of FG-CNTRC Timoshenko beams, Ke et al. [6] employed Ritz method to derive the governing equation from which the nonlinear frequencies of FG-CNTRC beam could be obtained. Alibeigloo [1] developed three-dimensional theory of elasticity for investigating the static bending problem of FG-CNTRC plate with piezoelectric layers under uniform load for simply supported boundary conditions. By using the first-order shear deformation theory and element-free IMLS-Ritz, Zhang et al. [25] investigated the free vibration behaviours of FG-CNTRC triangular plates reinforced SWCNTs. Lei et al. [9] proposed an approach for the buckling analysis of FG-CNTRC plates by using the element-free kp-Ritz method with a set of mesh-free kernel particle functions.

Using the classical mechanics theories, the size-effect of nanoplates is not taken into account in analysing the behaviour of nanoplates. For this reason, researchers developed higher order continuum theories for capturing the size-effect of nanoplates [7, 10, 21, 22]. Among these theories, the modified couple stress (MCS) proposed by Yang et al. [23] is considered as simplest theory to capture the size-effect, because it contains only one material length scale parameter.

Hughes et al. [5] introduced an advanced numerical method so-called IsoGeometric Analysis (IGA) which combine the Computer Aided Design (CAD) and Finite Element Analysis (FEA). The non-uniform rational B-spline (NURBS) basic functions are employed to describe the accurate geometry domain of structure. Moreover, it is easy to increase the order of NURBS functions with the smoothness through knot insertion [3, 13]. IGA has been applied for the solution of the linear and non-linear problems of FG-CNTRC nanoplates [14, 15, 20]. Furthermore, there are no publications on using the refined plate theories (RPT) [11] based on MCS theory and NURBS basic functions for the analysis the size effect behaviours of FG-CNTRC nanoplates. In this paper, the bending behaviours of FG-CNTRC nanoplates are investigated by using RPT theory and IGA, while the size effects are capture based MCS theory. The weak form of static bending is derived using the Hamilton's principle. By comparing the results with references solutions through the numerical examples, the proposed method proves its accuracy and dependability.

2 Main Theories

2.1 Refined Plated Theory

Based on Reddy's theory [17], which contains five unknowns, the four-variable RPT theory was proposed by Senthilnathan [11] such as:

$$\begin{aligned} u(x,y,z) &= u_0(x,y) - zw_{b,x}(x,y) + g(z)w_{s,x}(x,y) \\ v(x,y,z) &= v_0(x,y) + zw_{b,y}(x,y) + g(z)w_{s,y}(x,y) \\ w(x,y,z) &= w_b(x,y) + w_s(x,y) \end{aligned} \tag{1}$$

In Eq. (1), for depiction the spreading of transverse shear stress and strains across the thickness direction, the function $g(z) = f(z) - z$ is taken in the function $u(x, y, z)$

and $v(x,y,z)$, in which, the function $f(z) = -8z + 10z^3/h^2 + (6z^5)/(5h^4) + (8z^7)/(7h^6)$ [12] is satisfying the traction-free condition at the top and bottom surfaces ($z = \pm h/2$). Moreover, there is no requirement to use the shear correction factor for RPT theory.

From Eq. (1), the strain-displacement relations can be expressed as:

$$\begin{aligned} \varepsilon_b &= \varepsilon_o + z\kappa_1 + g\kappa_2 \\ \gamma &= f'\varepsilon_s \end{aligned} \tag{2}$$

where

$$\begin{aligned} \varepsilon_b &= \begin{Bmatrix} \varepsilon_{xx} \\ \varepsilon_{yy} \\ \gamma_{xy} \end{Bmatrix}; \ \varepsilon_o = \begin{Bmatrix} u_{0,x} \\ v_{0,y} \\ u_{0,y} + v_{0,x} \end{Bmatrix}; \ \kappa_1 = -\begin{Bmatrix} w_{b,xx} \\ w_{b,yy} \\ 2w_{b,xy} \end{Bmatrix}; \\ \kappa_2 &= \begin{Bmatrix} w_{s,xx} \\ w_{s,yy} \\ 2w_{s,xy} \end{Bmatrix}; \ \gamma = \begin{Bmatrix} \gamma_{xz} \\ \gamma_{yz} \end{Bmatrix}; \ \varepsilon_s = \begin{Bmatrix} w_{s,x} \\ w_{s,y} \end{Bmatrix} \end{aligned} \tag{3}$$

2.2 Modified Couple Stress Theory

To capture the size-effect of nano-plates, the modified couple stress theory proposed by Yang et al. [23] is used. The virtual strain energy contain not only the symmetric tensor σ_{ij} but also the deviatoric part of symmetric couple stress tensor m_{ij} such as:

$$\delta U = \int_V (\sigma_{ij}\delta\varepsilon_{ij} + m_{ij}\delta\chi_{ij})dV \tag{4}$$

in which, ε_{ij} are components of Green-Lagrange strain tensor; χ_{ij} are the components of the symmetric curvature tensor m_{ij}.

According to Eq. (1), the components of the rotation vector are given by:

$$\begin{aligned} \theta_x &= \tfrac{1}{2}\left(\tfrac{\partial w}{\partial y} - \tfrac{\partial v}{\partial z}\right) = \tfrac{1}{2}\left(2w_{b,y} + 2w_{s,y} - f'(z)w_{s,y}\right) \\ \theta_y &= \tfrac{1}{2}\left(\tfrac{\partial u}{\partial z} - \tfrac{\partial w}{\partial x}\right) = \tfrac{1}{2}\left(-2w_{b,x} - 2w_{s,x} + f'(z)w_{s,x}\right) \\ \theta_z &= \tfrac{1}{2}\left(\tfrac{\partial v}{\partial x} - \tfrac{\partial u}{\partial y}\right) = \tfrac{1}{2}\left(v_{0,x} - u_{0,y}\right) \end{aligned} \tag{5}$$

and the components of curvature vector take the form as:

$$\begin{aligned} \chi^b &= \chi_1^b + f'(z)\chi_2^b \\ \chi_1^b &= \tfrac{1}{2}\begin{Bmatrix} 2w_{b,xy} + 2w_{s,xy} \\ -2w_{b,xy} - 2w_{s,xy} \\ \left(w_{b,yy} - w_{b,xx}\right) + \left(w_{s,yy} - w_{s,xx}\right) \end{Bmatrix}; \chi_2^b = \tfrac{1}{4}\begin{Bmatrix} -4w_{s,xy} \\ 4w_{s,xy} \\ -2\left(w_{s,yy} - w_{s,xx}\right) \end{Bmatrix} \\ \chi^s &= \chi_0^s + f''(z)\chi_1^s \\ \chi_0^s &= \tfrac{1}{4}\begin{Bmatrix} v_{0,xx} - u_{0,xy} \\ v_{0,xy} - u_{0,yy} \end{Bmatrix}; \ \chi_2^s = \tfrac{1}{4}\begin{Bmatrix} -w_{s,y} \\ w_{s,x} \end{Bmatrix} \end{aligned} \tag{6}$$

The components of the deviatoric part of symmetric couple stress tensor can be present in a form as:

$$m_{ij} = 2G\ell^2\chi_{ij} \tag{7}$$

where, G denotes the shear module and ℓ is the material length scale parameter which is considered as a material property measuring the effect of couple stress.

2.3 Functionally Graded Carbon Nanotube-Reinforced Composites Plates

Figure 1 show four types of distributions of carbon nanotube (CNT): Uniform (UD) and functionally graded in the thickness direction of composite plate which are denoted as FG-V, FG-O, FG-X. According to the distributions of uniaxially aligned single-walled CNTs, the volume fraction V_{CNT} can be expressed as:

$$V_{CNT} = \begin{cases} V^*_{CNT} & \text{(UD)} \\ \left(1 + \frac{2z}{h}\right)V^*_{CNT} & \text{(FG-V)} \\ 2\left(1 - \frac{2|z|}{h}\right)V^*_{CNT} & \text{(FG-O)} \\ \frac{4|z|}{h}V^*_{CNT} & \text{(FG-X)} \end{cases} \tag{8}$$

in which

$$V^*_{CNT} = \frac{w_{CNT}}{w_{CNT} + (\rho_{CNT}/\rho_m) - (\rho_{CNT}/\rho_m)w_{CNT}} \tag{9}$$

where w_{CNT} is the mass fraction of the CNTs, ρ_{CNT} and ρ_m are densities of the CNTs and the matrix, respectively. By using Mori-Tanaka scheme or the rule of mixtures [18]. The effective mechanical properties of the CNT-reinforced composites plates can be estimated as follows:

$$\begin{aligned} E_{11} &= \eta_1 V_{CNT}E^{CNT}_{11} + V_m E^m \\ \frac{\eta_2}{E_{22}} &= \frac{V_{CNT}}{E^{CNT}_{22}} + \frac{V_m}{E^m} \\ \frac{\eta_3}{G_{12}} &= \frac{V_{CNT}}{G^{CNT}_{12}} + \frac{V_m}{G^m} \\ \rho &= \rho_{CNT}V_{CNT} + \rho_m V_m \end{aligned} \tag{10}$$

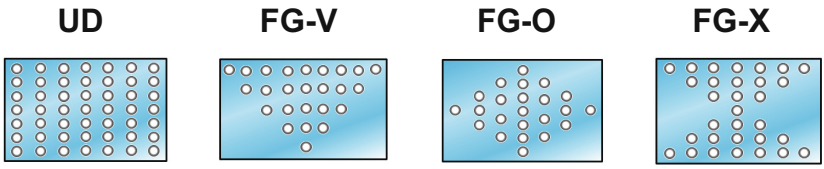

Fig. 1. Four distributions of CNT.

where the volume fraction of CNTs (V_{CNT}) and matrix (V_m) must be satisfy the following equation: $V_{CNT} + V_m = 1$. E^m, G^m are denote the Young's modulus and shear modulus of isotropic matrix, G_{12}^{CNT} corresponding to the shear modulus of CNT, material density is ρ; E_{11}^{CNT}, E_{22}^{CNT} are the Young's modulus of CNTs. In addition, the efficiency parameters η_1, η_2 and η_3 are introduced to account for the load transfer between CNTs and the matrix which are listed in Table 1 [18].

Table 1. The CNT efficiency parameters

V_{CNT}^*	η_1	η_2	η_3
0.110	0.149	0.934	0.934
0.140	0.150	0.941	0.941
0.170	0.140	1.381	1.381

In the same manner, the Poisson's ratio of the CNTRC nanoplate is defined as follow:

$$\upsilon_{12} = V_{CNT}^* \upsilon_{12}^{CNT} + V_m \upsilon^m \tag{11}$$

where υ_{12}^{CNT}, υ^m are the Poisson's ratio of CNT and the Poisson's ratio of matrix, respectively.

2.4 Weak Form of the Static Bending

By using the weak formulation, the weak form of the static bending analysis of CNTRC nanoplate subjected to transverse load q_0 based on MCS theory can be briefly expressed as:

$$\begin{aligned}&\int_{\Omega_e} (\delta\varepsilon_b)^T \mathbf{D}_u^b \varepsilon_b d\Omega_e + \int_{\Omega_e} (\delta\varepsilon_s)^T \mathbf{D}_u^s \varepsilon_s d\Omega_e + \int_{\Omega_e} \left(\delta\chi^b\right)^T \mathbf{D}_c^b diag\left(\Gamma_\chi^1\right)\chi^b d\Omega_e + \\ &\int_{\Omega_e} (\delta\chi^s)^T \mathbf{D}_c^s diag\left(\Gamma_\chi^2\right)\chi^s d\Omega_e = \int_{\Omega_e} \delta w q_0 d\Omega_e\end{aligned} \tag{12}$$

in which $diag\left(\Gamma_\chi^1\right) = diag(1,1,2)$ and $diag\left(\Gamma_\chi^2\right) = diag(2,2)$, the material matrices D_u^b, D_u^s, D_c^b and D_c^s are taken in the form such as:

$$\begin{aligned}&\mathbf{D}_u^b = \begin{bmatrix} \mathbf{A}^u & \mathbf{B}^u & \mathbf{E}^u \\ \mathbf{B}^u & \mathbf{D}^u & \mathbf{F}^u \\ \mathrm{E}^u & \mathbf{F}^u & \mathbf{H}^u \end{bmatrix}; \mathbf{D}_u^s = \int_{-h/2}^{h/2} \left(f'(z)^2\right) \begin{bmatrix} Q_{44} & 0 \\ 0 & Q_{55} \end{bmatrix} dz \\ &\mathbf{D}_c^b = \begin{bmatrix} \mathbf{A}^c & \mathbf{B}^c \\ \mathbf{B}^c & \mathbf{E}^c \end{bmatrix}; \mathbf{D}_c^s = \begin{bmatrix} \mathbf{X}^c & \mathbf{Y}^c \\ \mathbf{Y}^c & \mathbf{Z}^c \end{bmatrix}\end{aligned} \tag{13}$$

where the material matrices can be defined as:

$$
\begin{aligned}
&(\mathbf{A}^u, \mathbf{B}^u, \mathbf{D}^u, \mathbf{E}^u, \mathbf{F}^u, \mathbf{H}^u) = \int_{-h/2}^{h/2} \left(1, z, z^2, g(z), zg(z), g(z)^2\right) \begin{bmatrix} Q_{11} & Q_{12} & 0 \\ Q_{21} & Q_{22} & 0 \\ 0 & 0 & Q_{66} \end{bmatrix} dz \\
&(\mathbf{A}^c, \mathbf{B}^c, \mathbf{E}^c) = \int_{-h/2}^{h/2} \left(1, f'(z), [f'(z)]^2\right) \begin{bmatrix} 2\mu\ell^2 & 0 & 0 \\ 0 & 2\mu\ell^2 & 0 \\ 0 & 0 & 2\mu\ell^2 \end{bmatrix} dz \\
&(\mathbf{X}^c, \mathbf{Y}^c, \mathbf{Z}^c) = \int_{-h/2}^{h/2} \left(1, f''(z), [f''(z)]^2\right) \begin{bmatrix} 2\mu\ell^2 & 0 \\ 0 & 2\mu\ell^2 \end{bmatrix} dz \\
&Q_{11} = \tfrac{E_{11}}{1-\nu_{12}\nu_{21}},\ Q_{12} = \tfrac{\nu_{12}E_{22}}{1-\nu_{12}\nu_{21}},\ Q_{22} = \tfrac{E_{22}}{1-\nu_{12}\nu_{21}} \\
&Q_{66} = G_{12},\ Q_{55} = G_{13},\ Q_{44} = G_{23}
\end{aligned}
\tag{14}
$$

in which v_{12}, v_{21} are the effective Poisson's ratio, defined as the ratio of transverse strain to the axial strain and E_{11}, E_{22}, E_{33} are the Young's moduli of the CNTRC plates in the principal material coordinates and G_{12}, G_{13}, G_{23} are the effective shear moduli.

2.5 A Novel NURBS Formulation Based on Modified Couple Stress Theory

By using the NURBS basic function, the displacement field u of CNTRC nanoplate can be approximately expressed as:

$$\mathbf{u}^h(\xi, \eta) = \sum_{i=1}^{mxn} N_I(\xi, \eta)\mathbf{d}_I \tag{15}$$

where N_I is the shape function and $\mathrm{d_I} = [u_{0I}, v_{0I}, w_{bI}, w_{sI}]$ denotes the vector of degree of freedom associated with the control point I. The in-plane and shear strains can be obtained as:

$$\left[\boldsymbol{\varepsilon}_0^T, \boldsymbol{\kappa}_1^T, \boldsymbol{\kappa}_2^T, \boldsymbol{\varepsilon}_s^T\right]^T = \sum_{i=1}^{mxn} \left[\left(\mathbf{B}_I^m\right)^T, \left(\mathbf{B}_I^{b1}\right)^T, \left(\mathbf{B}_I^{b2}\right)^T, \mathbf{B}_I^s\right]^T \mathbf{d}_I \tag{16}$$

in which

$$
\begin{aligned}
&\mathbf{B}_I^m = \begin{bmatrix} N_{I,x} & 0 & 0 & 0 \\ 0 & N_{I,y} & 0 & 0 \\ N_{I,y} & N_{I,x} & 0 & 0 \end{bmatrix};\ \mathbf{B}_I^{b1} = -\begin{bmatrix} 0 & 0 & N_{I,xx} & 0 \\ 0 & 0 & N_{I,yy} & 0 \\ 0 & 0 & 2N_{I,xy} & 0 \end{bmatrix}; \\
&\mathbf{B}_I^{b2} = \begin{bmatrix} 0 & 0 & 0 & N_{I,xx} \\ 0 & 0 & 0 & N_{I,yy} \\ 0 & 0 & 0 & 2N_{I,xy} \end{bmatrix};\ \mathbf{B}_I^{s0} = \begin{bmatrix} 0 & 0 & 0 & N_{I,x} \\ 0 & 0 & 0 & N_{I,y} \end{bmatrix}
\end{aligned}
\tag{17}
$$

and the curvatures are

$$\left[\left(\boldsymbol{\chi}_1^b\right)^T,\left(\boldsymbol{\chi}_2^b\right)^T,\left(\boldsymbol{\chi}_0^s\right)^T,\left(\boldsymbol{\chi}_1^s\right)^T\right]^T=\sum_{i=1}^{mxn}\left[\left(\mathbf{B}_I^{\chi b1}\right)^T,\left(\mathbf{B}_I^{\chi b2}\right)^T,\left(\mathbf{B}_I^{\chi s0}\right)^T,\left(\mathbf{B}_I^{\chi s1}\right)^T\right]^T dI \tag{18}$$

where

$$\begin{aligned}
\mathbf{B}_I^{\chi b1}&=\tfrac{1}{2}\begin{bmatrix}0&0&2N_{I,xy}&2N_{I,xy}\\0&0&-2N_{I,xy}&-2N_{I,xy}\\0&0&\left(N_{I,yy}-N_{I,xx}\right)&\left(N_{I,yy}-N_{I,xx}\right)\end{bmatrix};\\
\mathbf{B}_I^{\chi b2}&=\tfrac{1}{4}\begin{bmatrix}0&0&0&-2N_{I,xy}\\0&0&0&2N_{I,xy}\\0&0&0&-\left(N_{I,yy}-N_{I,xx}\right)\end{bmatrix}\\
\mathbf{B}_I^{\chi s0}&=\tfrac{1}{4}\begin{bmatrix}-N_{I,xy}&N_{I,xx}&0&0\\-N_{I,yy}&N_{I,xy}&0&0\end{bmatrix};\ \mathbf{B}_I^{\chi s1}=\tfrac{1}{4}\begin{bmatrix}0&0&0&N_{I,y}\\0&0&0&N_{I,x}\end{bmatrix}
\end{aligned} \tag{19}$$

Substituting Eqs. (16) and (18) into Eq. (12), the matrix form of the global equilibrium equations for static bending of CNTRC nanoplate can be written as follows

$$\mathbf{Kd}=\mathbf{F} \tag{20}$$

in which $\mathbf{K}=\mathbf{K}^u+\mathbf{K}^\theta$ is the global stiffness matrix; $\mathbf{K}^u$, $\mathbf{K}^\theta$ are the stiffness matrix corresponding to the classical mechanic theory and the couple stress theory. These matrix are computed by:

$$\begin{aligned}
\mathbf{K}^u&=\int_\Omega\left[\begin{Bmatrix}\mathbf{B}^m\\\mathbf{B}^{b1}\\\mathbf{B}^{b2}\end{Bmatrix}^T\begin{bmatrix}\mathbf{A}^u&\mathbf{B}^u&\mathbf{E}^u\\\mathbf{B}^u&\mathrm{D}^u&\mathbf{F}^u\\\mathbf{E}^u&\mathbf{F}^u&\mathbf{H}^u\end{bmatrix}\begin{Bmatrix}\mathbf{B}^m\\\mathbf{B}^{b1}\\\mathbf{B}^{b2}\end{Bmatrix}+\left(\mathbf{B}^s\right)^T\mathbf{D}_u^s\mathbf{B}^s\right]d\Omega\\
\mathbf{K}^\theta&=\int_\Omega\left[\begin{Bmatrix}\boldsymbol{\chi}_1^b\\\boldsymbol{\chi}_2^b\end{Bmatrix}^T\begin{bmatrix}\mathbf{A}^c&\mathbf{B}^c\\\mathbf{B}^c&\mathbf{E}^c\end{bmatrix}\begin{Bmatrix}\boldsymbol{\chi}_1^b\\\boldsymbol{\chi}_2^b\end{Bmatrix}+\begin{Bmatrix}\boldsymbol{\chi}_0^s\\\boldsymbol{\chi}_1^s\end{Bmatrix}^T\begin{bmatrix}\mathbf{X}^c&\mathbf{Y}^c\\\mathbf{Y}^c&\mathbf{Z}^c\end{bmatrix}\begin{Bmatrix}\boldsymbol{\chi}_0^s\\\boldsymbol{\chi}_1^s\end{Bmatrix}\right]d\Omega
\end{aligned} \tag{21}$$

and the load vector can be expressed as:

$$\mathbf{F}=\int_\Omega q_0\mathbf{R}d\Omega;\quad \mathbf{R}_I=[0,0,N_I,N_I]^T \tag{22}$$

3 Numerical Examples

In this section, several numerical examples are presented with the following aims:

(1) Confirming the accuracy of the proposed approach presented in Sect. 2 by comparing its results with those in analytical solution [19].

(2) Investigating the size effect behaviours on the static bending of CNTRC nanoplate with difference thicknesses of plate by changing the material length scale parameter.

3.1 Example 1

The cubic NURBS function with the element mesh of 9×9 is sufficient for all numerical examples in this paper. For verification studies, the material properties of all edges simply support (SSSS) homogenous square plates are chosen as: $E = 1.44$ GPa, $\nu = 0.3$. The non-dimensional deflection of plates $\bar{w} = (10wEh^3)/(q_0a^4)$ under a sinusoidally distributed load $q_0 \sin(\pi x/a) \sin(\pi y/a)$ are compared with the Navie analytical solutions [19] and a numerical solution [21] with six different values of material length scale ratio $(\ell/h = 0,\ 0.2, 0.4, 0.6, 0.8,\ 1)$ and the results match very well with reference solutions. It is clearly that, the length scale ratio $\ell/h = 0$ indicates the plates with no size-effect and the present model get back the classical model.

Further verification of accuracy of present model is performed on SSSS functionally graded (FG) square microplates with difference length-thickness ratio under sinusoidal load. The FG plate is made of alumina (Al - material 1), aluminium (Al2O3 - material 2) and the material properties are chosen such as: E_1 = 380 GPa; ρ_1 = 3800 kg/m^3; E_2 = 70 GPa; ρ_2 = 2702 kg/m^3, and Poisson's ratio is constant through the thickness of plate with its value is equal to 0.3. In Tables 2 and 3, the non-dimensional deflections of thick plates are little bit smaller than analytical solution [19] (1.87% for n = 0 and 1.57% for n = 5, 10), and there is no difference between proposed model and other references solutions for thin plates. It clearly noticed that the two above examples prove the accuracy and conformability of proposed model.

Table 2. Non-dimensional central deflection of SSSS homogeneous plates

ℓ/h	$a/h = 5$			$a/h = 20$			$a/h = 100$		
	Ref. [19]	Ref. [21]	Present	Ref. [19]	Ref. [21]	Present	Ref. [19]	Ref. [21]	Present
0	0.3433	0.3433	0.3433	0.2842	0.2842	0.2842	0.2804	0.2804	0.2804
0.2	0.275	0.2875	0.2862	0.2430	0.243	0.2429	0.2401	0.2401	0.2401
0.4	0.1934	0.1934	0.1912	0.1693	0.1693	0.1691	0.1677	0.1677	0.1677
0.6	0.1251	0.1251	0.1232	0.1124	0.1124	0.1123	0.1116	0.1116	0.1116
0.8	0.0838	0.0838	0.0823	0.0765	0.0765	0.0764	0.0760	0.076	0.0760
1	0.0588	0.0588	0.0577	0.0542	0.0542	0.0541	0.0539	0.0539	0.0539

3.2 Example 2

The material properties of the matrix of FG-CNTRC nanoplates are assumed to be $E^m = 2.1$ GPa , $\nu^m = 0.34$, $\rho^m = 1160$ kg/m^3 at the room temperature (300 K) and the material properties of single wall CNTs can be taken as follows: $E_{11}^{CNT} = 5.6466$ TPa, $E_{22}^{CNT} = 7.08$ TPa, $G_{12}^{CNT} = 1.9445$ TPa, $\alpha_{11}^{CNT} = 3.4584 \quad 10^{-6}/\text{K}$, $\alpha_{22}^{CNT} = \quad 5.1682$

Table 3. Non-dementional deflection of SSSS AL/AL2O3 square microplates (rule of mixtures scheme)

a/h	ℓ/h	n = 0			n = 5			n = 10		
		Ref. [19]	Ref. [20]	Present	Ref. [19]	Ref. [20]	Present	Ref. [19]	Ref. [20]	Present
5	0	0.3433	0.3433	0.3433	1.0885	1.0885	1.0877	1.2276	1.2276	1.2270
	0.2	0.2875	0.2875	0.2862	0.8981	0.8981	0.8926	1.0247	1.0247	1.0184
	0.4	0.1934	0.1934	0.1912	0.5925	0.5925	0.5850	0.6908	0.6908	0.6818
	0.6	0.1251	0.1251	0.1232	0.3802	0.3802	0.3745	0.4514	0.4514	0.4443
	0.8	0.0838	0.0838	0.0823	0.2539	0.2539	0.2500	0.3052	0.3052	0.3003
	1	0.0588	0.0588	0.0577	0.1782	0.1782	0.1754	0.2158	0.2158	0.2124
10	0	0.2961	0.2961	0.2960	0.9114	0.9114	0.9111	1.0087	1.0087	1.0085
	0.2	0.2520	0.2520	0.2517	0.7743	0.7743	0.7730	0.8697	0.8697	0.8682
	0.4	0.1742	0.1742	0.1736	0.5349	0.5349	0.5331	0.6175	0.6175	0.6153
	0.6	0.1150	0.1150	0.1145	0.3538	0.3538	0.3524	0.4177	0.4177	0.4159
	0.8	0.0780	0.0780	0.0776	0.2403	0.2403	0.2393	0.2879	0.2879	0.2866
	1	0.0552	0.0552	0.0549	0.1702	0.1702	0.1695	0.2058	0.2058	0.2050
20	0	0.2842	0.2842	0.2842	0.8669	0.8669	0.8668	0.9538	0.9538	0.9537
	0.2	0.2430	0.2430	0.2429	0.7429	0.7429	0.7425	0.8303	0.8303	0.8299
	0.4	0.1693	0.1693	0.1691	0.5201	0.5201	0.5196	0.5986	0.5986	0.5980
	0.6	0.1124	0.1124	0.1123	0.3470	0.3470	0.3466	0.4090	0.4090	0.4085
	0.8	0.0765	0.0765	0.0764	0.2368	0.2368	0.2365	0.2834	0.2834	0.2831
	1	0.0542	0.0542	0.0541	0.1681	0.1681	0.1680	0.2033	0.2033	0.2030
100	0	0.2804	0.2804	0.2804	0.8527	0.8527	0.8526	0.9362	0.9362	0.9361
	0.2	0.2401	0.2401	0.2401	0.7327	0.7327	0.7327	0.8176	0.8176	0.8176
	0.4	0.1677	0.1677	0.1677	0.5153	0.5153	0.5153	0.5925	0.5925	0.5924
	0.6	0.1116	0.1116	0.1116	0.3448	0.3448	0.3448	0.4061	0.4061	0.4061
	0.8	0.0760	0.0760	0.0760	0.2357	0.2357	0.2356	0.2820	0.2820	0.2820
	1	0.0539	0.0539	0.0539	0.1675	0.1675	0.1675	0.2024	0.2024	0.2024

$10^{-6}/\mathrm{K}$. The values of the CNT efficiency parameters for three case of V^*_{CNT} are taken in Table 1. Moreover, we assume that $G_{23} = G_{13} = G_{12}$ and $\eta_3 = \eta_2$.

In the Table 4, the non-dimensional central deflection of SSSS FG-CNTRC nanoplates under uniform loads for classical model are compare with the solutions obtained by the FE commercial package ANSYS [26] and the numerical method in Ref. [21]. It can be seen that the present results are in good agreement with those reference solutions. In addition, Table 4 shows that the deflection for FG-O plate is the largest but it is the smallest for FG-X plate in case for simply support boundary condition.

Table 4. Non-dimensional deflection of FG-CNTRC plates (SSSS)

V^*_{CNT}	a/h	Types	Ref. [26]	Ref. [20]	Present
0.11	50	UD	1.155	1.157	1.1417
		FG-V	1.652	1.654	1.6411
		FG-O	2.15	2.162	2.1477
		FG-X	0.792	0.792	0.7767
	20	UD	0.03629	0.0363	0.03395
		FG-V	0.04876	0.04882	0.04673
		FG-O	0.0613	0.06233	0.06006
		FG-X	0.02696	0.02696	0.02458
0.14	50	UD	0.918	0.916	0.9012
		FG-V	1.326	1.322	1.308
		FG-O	1.738	1.736	1.721
		FG-X	0.628	0.627	0.612
	20	UD	0.03001	0.02992	0.02760
		FG-V	0.04025	0.04015	0.03801
		FG-O	0.0507	0.0512	0.04887
		FG-X	0.02258	0.02256	0.02023
0.17	50	UD	0.752	0.753	0.744
		FG-V	1.081	1.083	1.075
		FG-O	1.411	1.417	1.410
		FG-X	0.514	0.516	0.506
	20	UD	0.02349	0.0235	0.02203
		FG-V	0.03171	0.03178	0.03048
		FG-O	0.04007	0.04054	0.03916
		FG-X	0.01738	0.01752	0.01599

In the next step, the effects of material length scale parameter on central deflection of FG-CNTRC nanoplates are studied by increasing the parameter. Tables 5, 6 and 7 present the non-dimensional deflection of FG-CNTRC nanoplates by changing length scale ratio. It is observed that the non-dimensional deflection decrease when the ratio increase. In the other words, the higher ratio is chosen, the lower nanoplate's central deflection as well as the thinner the nanoplate, the higher nanoplate's stiffness.

Table 5. Non-dimensional deflection of FG-CNTRC plates ($V^*_{CNT} = 0.11$)

a/h	Types	ℓ/h					
		0	0.2	0.4	0.6	0.8	1
20	UD	0.03395	0.03322	0.03126	0.02864	0.02578	0.02295
	FG-V	0.04673	0.04553	0.04231	0.03795	0.03328	0.02881
	FG-O	0.06006	0.05827	0.05339	0.04685	0.04005	0.03380
	FG-X	0.02458	0.02398	0.02255	0.02084	0.01909	0.01739
50	UD	1.14174	1.13206	1.09700	1.03384	0.95090	0.85917
	FG-V	1.64107	1.61482	1.53263	1.40304	1.24916	1.09243
	FG-O	2.14771	2.09937	1.95599	1.74495	1.51055	1.28598
	FG-X	0.77672	0.77297	0.75865	0.73046	0.69000	0.64157

Table 6. Non-dimensional deflection of FG-CNTRC plates ($V^*_{CNT} = 0.14$)

a/h	Types						
		0	0.2	0.4	0.6	0.8	1
20	UD	0.02760	0.02702	0.02550	0.02352	0.02139	0.01928
	FG-V	0.03801	0.03712	0.03474	0.03152	0.02803	0.02461
	FG-O	0.04887	0.04762	0.04414	0.03933	0.03418	0.02931
	FG-X	0.02023	0.01966	0.01840	0.01700	0.01565	0.01437
50	UD	0.90127	0.89615	0.87563	0.83550	0.77976	0.71539
	FG-V	1.30856	1.29281	1.24047	1.15292	1.04387	0.92823
	FG-O	1.72141	1.69178	1.59809	1.45139	1.28018	1.10920
	FG-X	0.61213	0.60965	0.60074	0.58311	0.55686	0.52422

Table 7. Non-dimensional deflection of FG-CNTRC plates ($V^*_{CNT} = 0.17$)

a/h	Types						
		0	0.2	0.4	0.6	0.8	1
20	UD	0.02203	0.02155	0.02027	0.01854	0.01665	0.01479
	FG-V	0.03048	0.02968	0.02751	0.02459	0.02148	0.01852
	FG-O	0.03916	0.03799	0.03476	0.03040	0.02587	0.02173
	FG-X	0.01599	0.01556	0.01457	0.01342	0.01227	0.01115
50	UD	0.74405	0.73736	0.71344	0.67085	0.61542	0.55455
	FG-V	1.07512	1.05669	0.99979	0.91137	0.80765	0.70314
	FG-O	1.40881	1.37575	1.27770	1.13431	0.97667	0.82723
	FG-X	0.50613	0.50307	0.49244	0.47279	0.44535	0.41294

4 Conclusions

In this paper, the refined plate theory (RPT) based the NURBS basic function has been developed to investigated the small scale effect behaviours on static bending of functionally graded carbon nanotube-reinforced composite nanoplates (FG-CNTRC) by using modified couple stress theory (MCT) with only one material length scale parameter. By using RPT theory with four unknowns, there no need to use shear correction factor and the proposed model is able to accurately capture the central deformations of FG-CNTRC nanoplates. Numerical examples show the exactness and efficiency of the proposed approach through comparison with the difference reference solutions. For studying the small scale effect of FG-CNTRC nanoplates, the deflections of plates are calculated for different small scale ratio's ℓ/h. The results also indicate that the thinner the FG-CNTRC nanoplate the higher nanoplate's stiffness.

Acknowledgement. The authors would like to acknowledge the MaDurOS project and the support from DeMoPreCI-MDT SIM SBO.

References

1. Alibeigloo, A.: Static analysis of functionally graded carbon nanotube-reinforced composite plate embedded in piezoelectric layers by using theory of elasticity. Compos. Struct. **95**, 612–622 (2013)
2. Khan, U., Coleman, J.N., Blau, W.J., Gun'ko, Y.K.: YK. Carbon Small but strong: a review of the mechanical properties of carbon nanotubepolymer composites **44**(9), 1624–1652 (2006)
3. Cottrell, J.A., Reali, A., Bazilevs, Y., Hughes, T.J.R.: Isogeometric analysis of structural vibrations. Comput. Methods Appl. Mech. Eng. **195**(41), 5257–5296 (2006)
4. Esawi, A.M.K., Farag, M.: Carbon nanotube reinforced composites: potential and current challenges. Mater. Des. **28**(9), 2394–2401 (2007)
5. Hughes, T.J.R., Cottrell, J.A., Bazilevs, Y.: Isogeometric analysis: CAD, finite elements, NURBS, exact geometry and mesh refinement. Comput. Methods Appl. Mech. Eng. **194** (39), 4135–4195 (2005)
6. Ke, Liao-Liang, Yang, Jie, Kitipornchai, Sritawat: Nonlinear free vibration of functionally graded carbon nanotube-reinforced composite beams. Compos. Struct. **92**(3), 676–683 (2010)
7. Koiter, W.T.: Couple stresses in the theory of elasticity, I and II Nederl. Akad. Wetensch. Proc. Ser **B67**, 17–44 (1964)
8. Gu, C., Lau, Kt: A critical review on nanotube and nanotube/nanoclay related polymer composite materials. Compos. B Eng. **37**(6), 425–436 (2006)
9. Lei, Z.X., Liew, K.M., Yu, J.L.: Buckling analysis of functionally graded carbon nanotube-reinforced composite plates using the element-free kp-Ritz method. Compos. Struct. **98**, 160–168 (2013)
10. Mindlin, R.D.: Influence of couple-stresses on stress concentrations. Exp. Mech. **3**(1), 1–7 (1963)
11. Lim, S.P., Senthilnathan, N.R., Lee, K.H., Chow, S.T.: Buckling of shear-deformable plates. AIAA J. **25**(9), 1268–1271 (1987)
12. Nguyen, Hoang X., Nguyen, Tuan N., Abdel-Wahab, M., Bordas, S.P.A., Nguyen-Xuan, H., Vo, T.P.: A refined quasi-3D isogeometric analysis for functionally graded microplates based on the modified couple stress theory. Comput. Methods Appl. Mech. Eng. **313**, 904–940 (2017)
13. Nguyen, V.P., Nguyen-Xuan, H.: High-order B-splines based finite elements for delamination analysis of laminated composites. Compos. Struct. **102**, 261–275 (2013)
14. Phung-Van, Phuc, Abdel-Wahab, Magd, Liew, K.M., Bordas, S.P.A., Nguyen-Xuan, H.: Isogeometric analysis of functionally graded carbon nanotube-reinforced composite plates using higher-order shear deformation theory. Compos. Struct. **123**, 137–149 (2015)
15. Phung-Van, Lieu, Phuc, Q.X., Nguyen-Xuan, H., Wahab, M.A.: Size-dependent isogeometric analysis of functionally graded carbon nanotube-reinforced composite nanoplates. Compos. Struct. **166**, 120–135 (2017)
16. Rashidifar, M.A., Ahmadi, D.: Vibration analysis of randomly oriented carbon nanotube based on FGM beam using timoshenko theory. Adv. Mech. Eng. **7**(2), 653950 (2015)
17. Reddy, J.N.: A simple higher-order theory for laminated composite plates. J. Appl. Mech. **51** (4), 745–752 (1984)
18. Shen, H.-S., Zhang, C.-L.: Thermal buckling and postbuckling behavior of functionally graded carbon nanotube-reinforced composite plates. Mater. Des. **31**(7), 3403–3411 (2010)
19. Thai, Huu-Tai, Kim, Seung-Eock: A size-dependent functionally graded Reddy plate model based on a modified couple stress theory. Compos. B Eng. **45**(1), 1636–1645 (2013)

20. Thanh, C.-L., Phung-Van, P., Thai, C.H., Nguyen-Xuan, H., Wahab, M.A.: Isogeometric analysis of functionally graded carbon nanotube reinforced composite nanoplates using modified couple stress theory. Compos. Struct. **184**, 633–649 (2018)
21. Richard, A.: Toupin, elastic materials with couple-stresses. Arch. Ration. Mech. Anal. **11**(1), 385–414 (1962)
22. Chong, A.C.M., Yang, F., Lam, D.C.C., Tong, P.: Couple stress based strain gradient theory for elasticity. Int. J. Solids Struct. **39**, 2731–2743 (2002)
23. Yang, F., Chong, A.C.M., Lam, D.C.C., Tong, P.: Couple stress based strain gradient theory for elasticity. Int. J. Solids Struct. **39**(10), 2731–2743 (2002)
24. Yas, M.H., Samadi, N.: Free vibrations and buckling analysis of carbon nanotube-reinforced composite Timoshenko beams on elastic foundation. Int. J. Press. Vessels Pip. **98**, 119–128 (2012)
25. Zhang, L.W., Lei, Z.X., Liew, K.M.: Free vibration analysis of functionally graded carbon nanotube-reinforced composite triangular plates using the FSDT and element-free IMLS-Ritz method. Compos. Struct. **120**, 189–199 (2015)
26. Zhu, P., Liew, K.M.: Static and free vibration analyses of carbon nanotube-reinforced composite plates using finite element method with first order shear deformation plate theory. Compos. Struct. **94**(4), 1450–1460 (2012)